

Uncertainty of three-nucleon continuum observables arising from uncertainties of two-nucleon potential parameters

Yu. Volkotrub, J. Golak, R. Skibiński, K. Topolnicki, and H. Witała

*M. Smoluchowski Institute of Physics,
Jagiellonian University, PL-30348 Kraków, Poland*

E. Epelbaum, H. Krebs, and P. Reinert

*Ruhr-Universität Bochum, Fakultät für Physik und Astronomie,
Institut für Theoretische Physik II, D-44780 Bochum, Germany*

(Dated: March 16, 2020)

Abstract

Propagation of uncertainties from two-nucleon potential parameters to three-nucleon observables, that is statistical errors for the neutron-deuteron elastic scattering and the deuteron breakup reaction at neutron laboratory energies up to 200 MeV is investigated. To that end we use the chiral nucleon-nucleon interaction with the semi-local momentum-space regularization at various orders of the chiral expansion, exploiting knowledge of the covariance matrix of its parameters. For both reactions we compare statistical uncertainties for chiral predictions with the uncertainties obtained in the same way but for the semi-phenomenological One-Pion-Exchange two-nucleon force. In addition for the elastic scattering we show also the truncation errors arising from restriction to a given order of chiral predictions, estimated among others within the Bayesian method, and the cutoff dependence of chiral predictions. We find that the resulting statistical uncertainty is smaller than the truncation errors for the chiral force at lower orders of the chiral expansion. At the higher orders of the chiral expansion and at low energies the statistical errors exceed the truncation ones but at intermediate and higher energies truncation errors are more important. Overall, magnitudes of the theoretical uncertainties are small and amount up to 0.5%-4%, depending on the observable and energy. We also find that the magnitudes of statistical uncertainties for the chiral and semi-phenomenological potentials are similar and that the dependence of predictions on the regularization parameter values is important at all investigated energies.

PACS numbers: 13.75.Cs, 21.45.-v, 25.10.+s

I. INTRODUCTION

The interactions between nucleons originate from interactions between quarks and gluons in the nonperturbative regime of Quantum Chromodynamics (QCD). Since currently the nuclear forces derived directly from QCD are not available, various effective models of nuclear interactions are used. In recent decades there has been increased interest in potentials based on the Chiral Effective Field Theory (χ EFT), linked to QCD and its symmetries. Within this approach it is possible to construct a consistent effective Hamiltonian with two- and many-body nuclear forces which incorporate all possible contributions up to a given order of the chiral expansion. Commonly nucleons and pions are chosen as relevant degrees of freedom, see Refs. [1–5] for more information on various chiral interactions.

Parallel to the development of the nuclear force models, the question how to estimate uncertainties of the calculated nuclear observables within a given model has arisen and various ideas for estimating theoretical uncertainties within the χ EFT framework, see Refs. [1, 4, 6–16] have been proposed and discussed. In the past, the uncertainty quantification of theoretical predictions in nuclear physics was treated with less care compared to the error analysis of experimental results. The estimation of uncertainties of theoretical predictions in few-nucleon systems was based mainly on comparison of predictions obtained using various models of the nuclear interaction. Such models describe, in *ab initio* calculations, low-energy observables with relatively high precision [17]. The CD-Bonn [18], the AV18 [19] or the chiral interactions derived by the Bochum-Bonn [6, 7, 10], the Moscow (Idaho)-Salamanca [20] or the Livermore [21, 22] groups, are good examples of such forces. Each of these models has some number of free parameters, whose values are fixed by the data. In the past, the authors of interaction models usually restricted themselves to determination of the values of the parameters but skipped their errors analysis, see for example Ref. [19]. The situation has changed since the Granada group revised the existing database for the nucleon-nucleon (NN) scattering and derived based on this data set the One-Pion-Exchange (OPE) Gaussian NN force model, Refs. [23, 24] and other potentials [25]. The careful statistical treatment applied during the fitting procedure allowed authors of Refs. [24, 25] to obtain the covariance matrix of the potential parameters. Using it, we studied the propagation of the uncertainties of the OPE-Gaussian potential parameters from the two-nucleon (2N) system to the elastic neutron-deuteron (nd) scattering observables in Ref. [26], determining for the first time in a quantitative way the corresponding theoretical uncertainties (called statistical uncertainties in the following). We refer the reader to Ref. [26] for a more general discussion on various types of theoretical uncertainties for the elastic nd scattering observables and to a special issue of *Journal of Physics G: Nuclear and Particle Physics* [16] for other observables and processes.

In this paper we show results for the elastic nd scattering and the neutron-induced deuteron breakup process obtained with the newest χ EFT family of potentials from the Bochum group [10]. For this interaction, derived completely up to the fifth order of the perturbative expansion (N^4 LO), the semi-local regularization in momentum space (SMS) has been applied. Further, for this potential the covariance matrix of its free parameters (obtained with the Granada database [24]) is known, which allows us to study, for the first time for a chiral force, the propagation of uncertainties of NN interaction parameters to three-nucleon (3N) continuum observables. Also the dependence of the uncertainty pattern on the order of the chiral expansion and on the regulator value is additionally studied.

On top of the statistical uncertainties, also the so-called truncation errors, which are un-

certainties arising from restriction to a given order of the chiral expansion can be evaluated. This was done for the first time in Ref. [6], where a simple prescription to estimate the truncation errors for the NN system was proposed. This prescription has been extended to many-nucleon systems in Ref. [8]. Though simple the algorithm of [6] does not give a statistical interpretation of truncation errors. Those can be estimated within Bayesian methods, see for example Refs. [13, 14] focused on NN observables. Recent papers [4, 12] have presented Bayesian results for truncation errors for observables in neutron-deuteron scattering below the pion production threshold. In the present paper we employ the Bayesian approach of Ref. [12] and compare resulting truncation errors to those obtained within the method from Ref. [8] as well as to the uncertainty due to the regulator dependence and the statistical errors.

This paper is organized as follows. In Sec. II we outline the Faddeev formalism for 3N calculations. In Sec. III we briefly describe our method used to estimate the propagation of the uncertainties of the potential parameters from the 2N system to the elastic 3N scattering observables. Sections IV and V describe results for elastic scattering and breakup reactions, respectively. Specifically, we discuss the theoretical statistical uncertainties and compare them with the truncation errors for a few chosen observables. We summarize in Sec. VI.

II. FORMALISM FOR 3N SCATTERING

The nucleon-deuteron scattering observables can be obtained using the formalism of the 3N Faddeev equation. This is one of the standard techniques to investigate 3N reactions and has been described in detail many times, see for example Refs. [27, 28, 30]. Thus we only briefly describe the key steps of this approach. The starting point for 3N calculations is solving the Lippmann-Schwinger equation with a given NN interaction V to get the NN t operator:

$$t = V + V\tilde{G}_0 t , \quad (2.1)$$

where \tilde{G}_0 is the free propagator of two nucleons. The t operator enters the 3N Faddeev scattering equation which, neglecting the 3N force, is written as:

$$T|\phi\rangle = tP|\phi\rangle + tPG_0T|\phi\rangle . \quad (2.2)$$

Here the initial state $|\phi\rangle$ is composed of the deuteron wave function and the momentum eigenstate of the projectile nucleon, G_0 is the free 3N propagator and P is the permutation operator $P \equiv P_{12}P_{23} + P_{13}P_{23}$ built from transpositions P_{ij} , which interchange particles i and j . Next the transition amplitudes, U for elastic Nd scattering and U_0 for the deuteron breakup process, are calculated via

$$\begin{aligned} \langle\phi'|U|\phi\rangle &= \langle\phi'|PG_0^{-1}|\phi\rangle + \langle\phi'|PT|\phi\rangle , \\ \langle\phi'|U_0|\phi\rangle &= \langle\phi'|(1+P)T|\phi\rangle \end{aligned} \quad (2.3)$$

and used to compute 3N scattering observables in the standard way [27]. $|\phi'\rangle$ in Eq. (2.3) denotes the suitable final two-body (nd) or three-body breakup state. In the latter case $|\phi'\rangle$ is a product of two relative-momentum eigenstates describing free motion of three outgoing nucleons.

In practice we work in the momentum-space partial wave basis $|p, q, \alpha\rangle$, where $p \equiv |\vec{p}|$ and $q \equiv |\vec{q}|$ are the magnitudes of the Jacobi momenta \vec{p} and \vec{q} ; α represents a set of

discrete quantum numbers for the 3N system in the jI -coupling, and is defined as $\alpha \equiv |(ls)j; (\lambda\frac{1}{2})I; (jI)JM_J; (t\frac{1}{2})TM_T\rangle$. Here l, s, j and t are the orbital angular momentum, total spin, total angular momentum, and total isospin of the $(2-3)$ subsystem. Further, λ is the orbital angular momentum of nucleon 1, which together with its spin $\frac{1}{2}$, couples to the total angular momentum I of nucleon 1. The angular momenta j and I couple to the total angular momentum of the 3N system J , and M_J denotes its projection on the quantization axis. The quantum numbers T and M_T describe the total isospin of the 3N system and its third component, respectively. Equation (2.2) is solved numerically by generating its Neumann series, which is subsequently summed up using the Padè method. For the investigations presented here we use all partial waves with $j \leq 5$ and $J \leq \frac{25}{2}$, which is sufficient to guarantee convergence of our predictions at the considered energies [27].

III. DETERMINATION OF THE STATISTICAL UNCERTAINTIES IN THE 3N SYSTEM

Computation of the above-defined statistical uncertainties for a specific observable requires a big sample of predictions obtained with different sets of parameters within a given model of the NN interaction. Prerequisite is the knowledge of the covariance matrix (or equivalently the correlation matrix) of the NN potential parameters, as is the case for the semilocally regularized in momentum space (SMS) chiral potential of Ref. [10]. We apply here the same method as was used previously in Ref. [26] to study the propagation of the uncertainties of the OPE-Gaussian potential parameters from the 2N system to 3N observables in elastic neutron-deuteron scattering. Therefore, we only briefly describe our algorithm to determine the statistical uncertainty and use it in the following for the chiral SMS force. Namely, given the expectation values (this set of potential parameters we call S_0 in the following), and correlation coefficients for the potential parameters, we sample, from the multivariate normal distribution, 50 sets of the potential parameters. For each set, we solve Eqs. (2.2)–(2.3) and compute 3N observables. Various possible estimators of the statistical uncertainties have been described in Ref. [26] and compared with each other. We use $\frac{1}{2}\Delta_{68\%}$ ¹ as an optimal measure for dispersion of predictions and consequently as an estimator of the statistical uncertainty at a given energy and a scattering angle. The same method was used to quantify the statistical error of the ³H binding energy in Ref. [32] and to estimate the uncertainties of the ⁴He bound states in Ref. [33]. Note that in the case of the SMS potential the regulator dependence and the availability of predictions at different orders of the chiral expansion increase the required number of computations substantially.

IV. RESULTS FOR THE ELASTIC Nd SCATTERING

We start presenting our results from discussing the dependence of statistical uncertainties, obtained with the chiral SMS NN interaction [10], on the order of the chiral expansion. This is done for selected observables in elastic neutron-deuteron (nd) scattering at three laboratory energies of the incoming neutron: $E = 65, 135$ and 200 MeV. We employ the regularization parameter $\Lambda = 450$ MeV. In Fig. 1 we show the quality of the elastic scattering

¹ $\Delta_{68\%}$ is the spread of results in the set of 34 (68% of 50) predictions based on different sets of the NN potential parameters. The set of 34 observables is constructed by discarding the 8 lowest and the 8 highest predictions for a given observable and at specific scattering angle and energy.

cross section data description obtained with the SMS chiral force. Our predictions are represented by bands which for each order of the chiral expansion cover a $\Delta_{68\%}$ estimator of the statistical uncertainty range. At the lowest energy, $E = 65$ MeV, predictions are very close to one another except for the NLO, which separates clearly at forward and backward scattering angles. The narrowness of bands clearly shows that at this energy the uncertainty of the nd elastic cross section arising from the uncertainty of the NN potential parameters is very small for all scattering angles. At two higher energies spreads of the different order of chiral expansion results become larger, however, the values of statistical uncertainties remain small. This is similar to the results for the OPE-Gaussian force [26], where small values of statistical uncertainties have been found for elastic nd scattering observables. The observed discrepancy with the proton-deuteron cross section data at small scattering angles is well understood as a result of neglecting the Coulomb force in our nd calculations [34]. The discrepancy around the minimum of the cross section is due to omitting 3N force contributions.

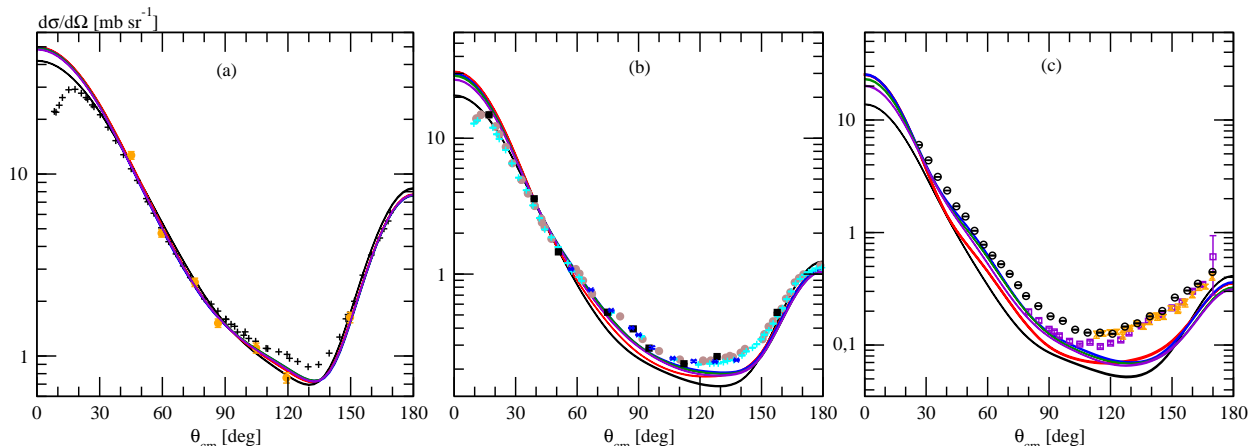


FIG. 1. (color online) The differential cross section $d\sigma/d\Omega$ for the elastic nd scattering process at the incoming neutron laboratory energy (a) $E = 65$ MeV, (b) $E = 135$ MeV and (c) $E = 200$ MeV as a function of the center-of-mass scattering angle $\theta_{c.m.}$. The black, red, blue, green and violet bands represent statistical uncertainties based on the chiral NLO, N^2 LO, N^3 LO, N^4 LO and N^4 LO+ ($\Lambda = 450$ MeV) SMS potentials, respectively. The experimental data are in: (a) from Ref. [35] (pd pluses) and [36] (nd orange circles), (b) from Ref. [37] (dp brown circles), Ref. [38] (dp cyan pluses), Ref. [39] (pd , $E = 135$ MeV, blue \times 's) and Ref. [39] (pd black squares), and in (c) from Ref. [40] (pd violet squares, $E = 198$ MeV), Ref. [41] (pd orange \times 's, $E = 180$ MeV), and Ref. [31] (pd black circles, $E = 198$ MeV).

In Fig. 2 we show the deuteron vector analyzing power iT_{11} . In this case, the chiral SMS interaction at the NLO order of chiral expansion fails to describe data at both higher energies. The statistical uncertainties remain small for all energies and orders and are negligible compared to differences between different order predictions at 200 MeV. In Fig. 3 we show the deuteron to neutron spin-transfer coefficient $K_y^y(d-n)$, for which the differences between predictions at various orders of the chiral expansion are especially big at 200 MeV. The statistical uncertainty obtained with the chiral N^2 LO force is relatively small at all energies and slightly grows with the increasing energy. For example, the difference between the two predictions obtained with the chiral N^2 LO and N^4 LO SMS potentials amounts

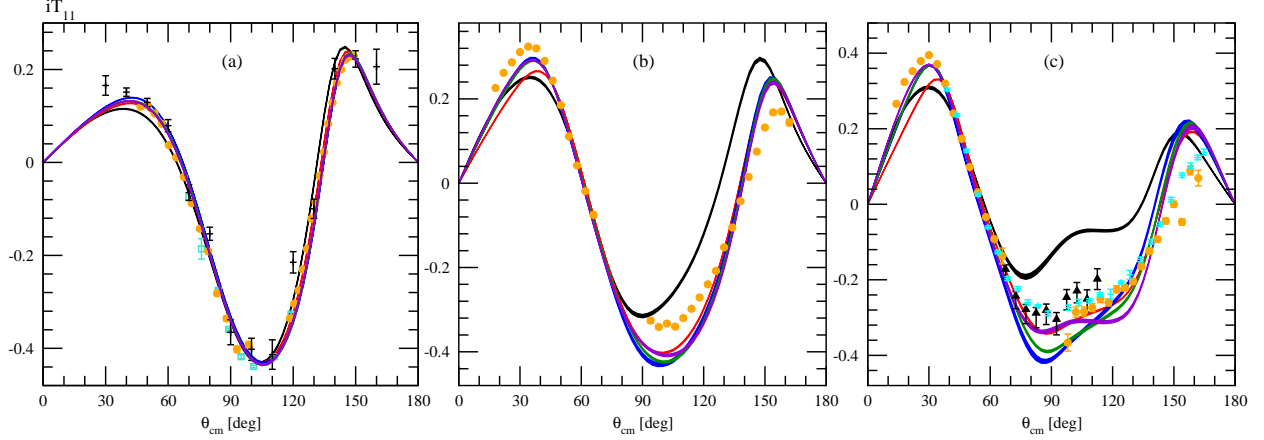


FIG. 2. (color online) The deuteron vector analyzing power iT_{11} for elastic nd scattering at the same energies as in Fig. 1 shown as a function of the scattering angle $\theta_{c.m.}$. For description of bands see Fig. 1. The data are in: (a) from Ref. [44] (pd pluses), Ref. [45] (pd orange circles), and Ref. [46] (pd cyan squares), (b) from Ref. [42] (pd orange circles), and (c) from Ref. [42] (pd orange circles), Ref. [43] (pd black up-triangles, $E = 197$ MeV), Ref. [29] (pd cyan pluses, $E = 186.6$ MeV).

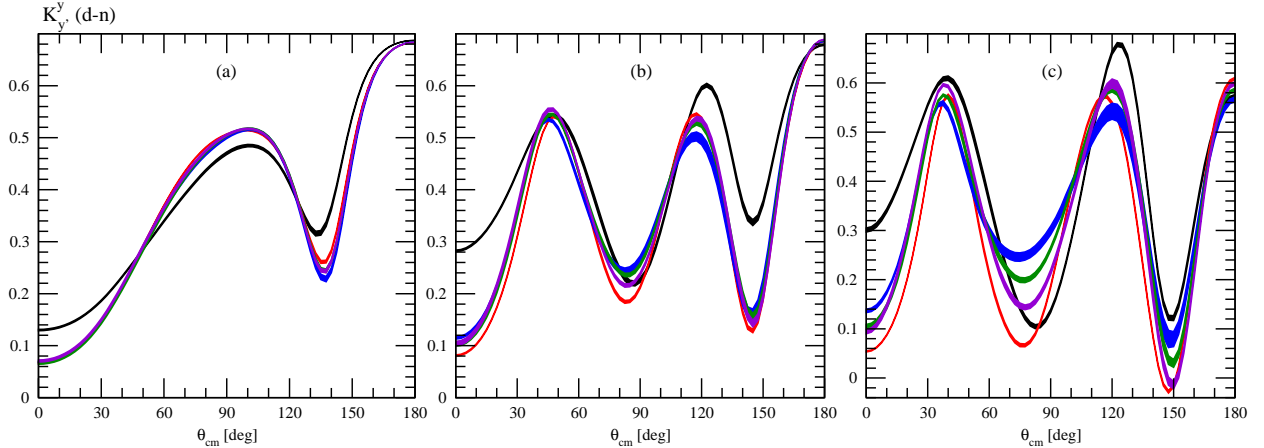


FIG. 3. (color online) The deuteron to neutron spin-transfer coefficient $K_{y'}^y(d-n)$ at the same energies as in Fig. 1 shown as a function of the scattering angle $\theta_{c.m.}$. For description of bands see Fig. 1.

$\approx 60\%$ at the minimum for 200 MeV at $\theta_{c.m.} = 147.5^\circ$, while the N²LO (N⁴LO) statistical uncertainties reach 0.27% (0.88%). In the case of the deuteron to neutron spin-transfer coefficient $K_{y'}^{yy}(d-n)$ shown in Fig. 4 we do not see such large statistical errors as in the case of $K_{y'}^y(d-n)$, but still their magnitude changes with the energy. Actually, we observe the following behavior: for the chiral SMS N²LO interaction the statistical uncertainty increases at $E = 135$ MeV compared to the $E = 65$ MeV, but at $E = 200$ MeV the statistical uncertainty decreases in the range of $\theta_{c.m.} \in [72.5^\circ, 150^\circ]$ compared to the $E = 135$ MeV case. For the chiral SMS N⁴LO interaction the statistical uncertainty decreases at $\theta_{c.m.} \in [40^\circ, 62.5^\circ] \cup [92.5^\circ, 112.5^\circ] \cup [145^\circ, 180^\circ]$ at $E = 135$ MeV compared to the energy 65 MeV and its magnitude further decreases at $\theta_{c.m.} \in [0^\circ, 47.5^\circ] \cup [92.5^\circ, 130^\circ]$ at $E = 200$

MeV compared to results at $E = 135$ MeV. To quantify this behaviour we give example at $\theta_{c.m.} = 145^\circ$ where the $\frac{1}{2}\Delta_{68\%}$ reaches 0.22%(0.24%), 0.30%(0.43%), and 0.27%(0.74%) of $K_{y'}^{yy}(\text{d-n})$ N²LO(N⁴LO) predictions at $E=65$ MeV, 135 MeV, and 200 MeV, respectively.

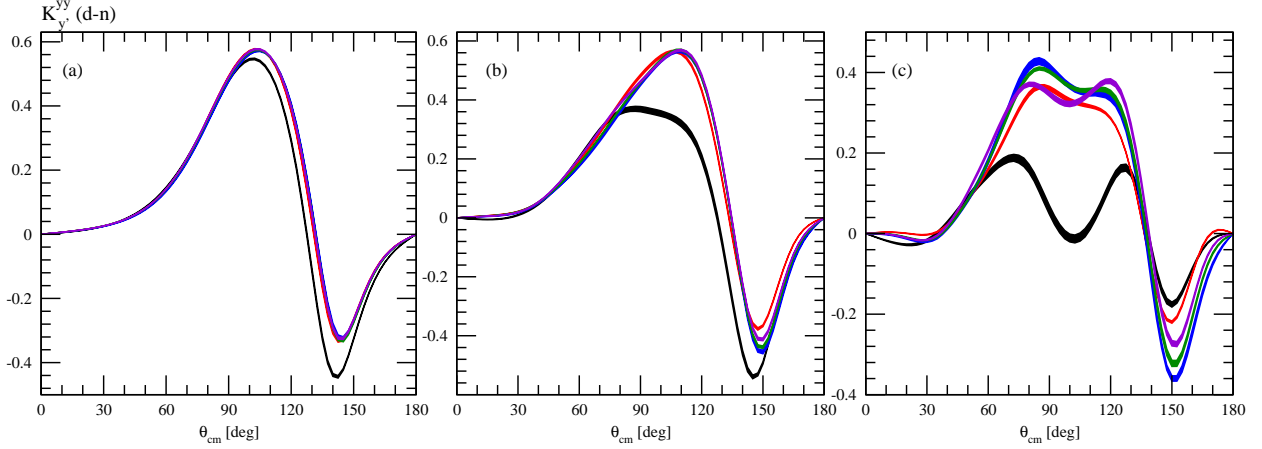


FIG. 4. (color online) The deuteron to neutron spin-transfer coefficient $K_{y'}^{yy}(\text{d-n})$ at the same energies as in Fig. 1 as a function of the scattering angle $\theta_{c.m.}$. Bands are as in Fig. 1.

It is interesting to compare magnitudes of the statistical errors with other kinds of theoretical uncertainties. Here, we would like to focus on the truncation errors present intrinsically in the chiral approach. Using the method from Ref. [8] we calculate the truncation error of a given 3N observable and compare its size with the statistical uncertainties already obtained. Namely, any 3N scattering observable X at a fixed cutoff value can be expanded up to the i -th order of the chiral expansion ($i = 0, 2, 3, \dots$) in the form

$$X = X^{(0)} + \Delta X^{(2)} + \Delta X^{(3)} + \dots + \Delta X^{(i)} \quad (4.1)$$

Then the truncation error $\delta(X)^{(i)}$ of an observable X at the i -th order of the chiral expansion with $i = 0, 2, 3, \dots$, is [8]

$$\begin{aligned} \delta(X)^{(0)} &\geq \max(Q^2|X^0|, |X^{(i \geq 0)} - X^{(j \geq 0)}|), \\ \delta(X)^{(2)} &\geq \max(Q^3|X^0|, Q|\Delta X^{(2)}|, |X^{(i \geq 2)} - X^{(j \geq 2)}|), \\ \delta(X)^{(i)} &\geq \max(Q^{i+1}|X^0|, Q^{i-1}|\Delta X^{(2)}|, Q^{i-2}|\Delta X^{(3)}|), i \geq 3 \end{aligned} \quad (4.2)$$

where $X^{(i)}$ denotes a prediction for the observable X at i -th order, $\Delta X^{(2)} \equiv X^{(2)} - X^{(0)}$ and $\Delta X^{(i)} \equiv X^{(i)} - X^{(i-1)}$ for $i \geq 3$. Further additional conditions $\delta(X)^{(2)} \geq Q\delta(X)^{(0)}$ and $\delta(X)^{(i)} \geq Q\delta(X)^{(i-1)}$ for $i \geq 3$ are imposed on the truncation errors. Such estimation of truncation errors accounts for the fact that the 3N force is neglected in the current investigation.

In Figs. 5 and 6 we show a comparison of the statistical and truncation errors for the deuteron vector analyzing power iT_{11} and the deuteron to neutron spin-transfer coefficient $K_{y'}^{yy}(\text{d-n})$. The N⁴LO SMS interaction with $\Lambda = 450$ MeV is used and the same energies are taken as in Fig. 1. For the sake of clarity, for the truncation errors we show only, with the blue curves, borders of the corresponding band.

In the case of the elastic deuteron vector analyzing power iT_{11} (Fig. 5) the relative difference between the widths of two bands of predictions i.e. $|\frac{1}{2}\Delta_{68\%} - \delta(X)^{(5)}|/(\frac{1}{2}(\frac{1}{2}\Delta_{68\%} +$

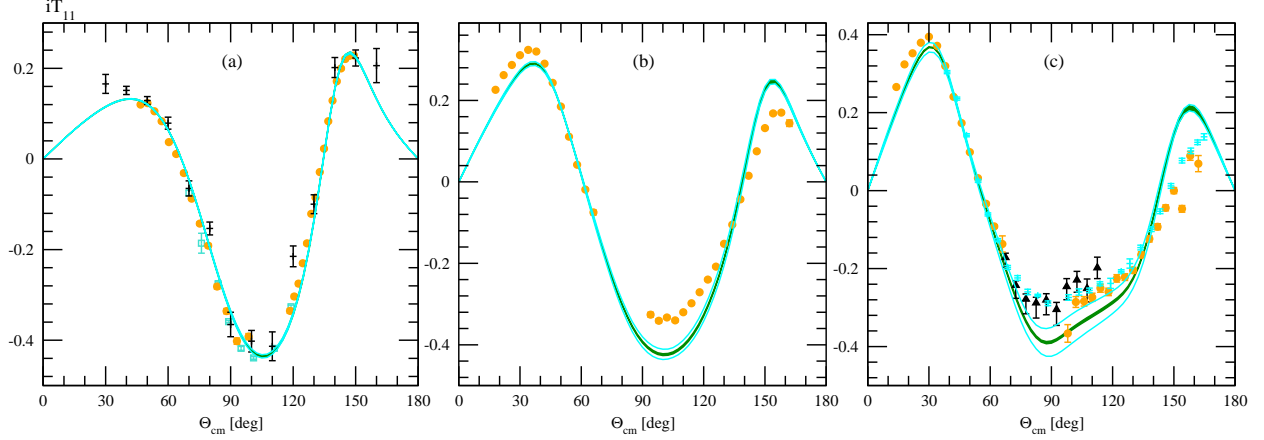


FIG. 5. (color online) The deuteron vector analyzing power iT_{11} for elastic nd scattering at the same energies as in Fig. 1 as a function of the scattering angle $\theta_{c.m.}$. The green solid band represents the statistical uncertainties based on the chiral N^4LO ($\Lambda = 450$ MeV) potential and the cyan lines represent the borders of the band for the truncation error for the same potential estimated using Eq.(4.2). The experimental data are the same as in Fig 2.

E [MeV]	$\theta_{c.m.}$ [deg]	$iT_{11}(S_0)$	$ iT_{11}(S_0) - iT_{11}^{min} $	$ iT_{11}^{max} - iT_{11}(S_0) $	$\frac{1}{2}\Delta_{68\%}$	$\delta(iT_{11})^{(5)}$
65	30	0.115234	0.000644	0.000493	0.000569	0.000425
	75	-0.117815	0.000820	0.000577	0.000699	0.001685
	120	-0.342291	0.002194	0.001620	0.001911	0.002680
	165	-0.089323	0.000486	0.000313	0.000399	0.000599
135	30	0.270409	0.001503	0.001204	0.001354	0.004570
	75	-0.233802	0.001052	0.001486	0.001269	0.009550
	120	-0.326824	0.003196	0.001554	0.002375	0.015205
	165	0.155717	0.001594	0.001174	0.001385	0.003405
200	30	0.367730	0.000706	0.001307	0.001007	0.012490
	75	-0.307313	0.002202	0.003750	0.002976	0.026585
	120	-0.286319	0.003595	0.002643	0.003119	0.028870
	165	0.175372	0.003484	0.002954	0.003219	0.007540

TABLE I. The deuteron analyzing power iT_{11} at given incoming neutron energy E and scattering angle $\theta_{c.m.}$, for the expectation values of the chiral SMS N^4LO potential parameters (denoted as set S_0), and its statistical $\frac{1}{2}\Delta_{68\%}$ as well as truncation $\delta^{(5)}$ errors. In addition, the borders of iT_{11} for 34 sets (iT_{11}^{min} and iT_{11}^{max}) are given. $\Delta_{68\%} \equiv iT_{11}^{max} - iT_{11}^{min}$.

$\delta(X)^{(5)})$ at $E = 65$ MeV reaches a few percent at scattering angle $\theta_{c.m.} = 90^\circ$. However, with increasing energy there is a significant increase in the magnitude of the truncation error which leads to an increase of the relative difference between the widths of two bands. For instance, at $E = 135$ MeV and $\theta_{c.m.} = 90^\circ$, that difference approaches about 84% (with $\Delta^{(5)} > \frac{1}{2}\Delta_{68\%}$), but already at $E = 200$ MeV it amounts to 92%. Similarly, for the deuteron to neutron spin-transfer coefficient $K_y^y(d-n)$, we observe at $\theta_{c.m.} = 90^\circ$ that at $E = 65$ MeV the difference between the statistical and truncation errors is almost invisible,

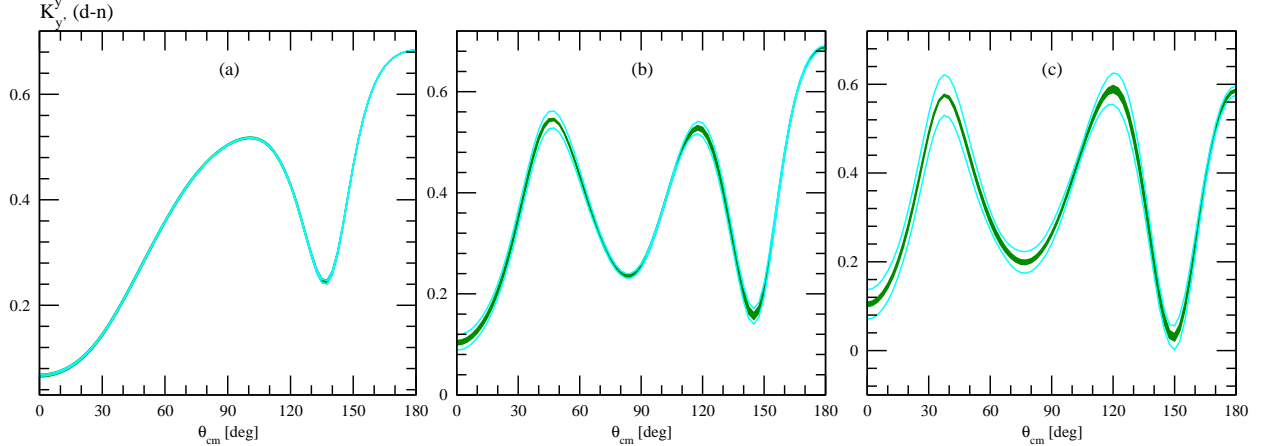


FIG. 6. (color online) The deuteron to neutron spin-transfer coefficient $K_{y'}^y(\text{d-n})$ for elastic nd scattering at the same energies as used in Fig. 1 as a function of the scattering angle $\theta_{c.m.}$. The band and lines are as in Fig. 5.

but at $E = 135$ MeV and $E = 200$ MeV it amounts up to 20% and 82%, respectively. Last but not least, we have to note that the ratios of the magnitude of the statistical uncertainties to the magnitude of the truncation error, that is $\frac{\frac{1}{2}\Delta_{68\%}}{\delta(X)^{(5)}}$, for the polarization observables are for most of the scattering angles much bigger than the same ratios but for the cross section. Probably this is due to a bigger sensitivity of polarization observables to the specific partial wave potential parameters of the chiral interaction used.

In Tab. I we give details on the statistical uncertainties and the truncation errors for the deuteron vector analyzing power iT_{11} shown in Fig. 5. Here, beside the predictions for iT_{11} obtained with the SMS N⁴LO potential we also show the magnitudes of the statistical uncertainties ($\frac{1}{2}\Delta_{68\%}$) and truncation errors ($\delta(X)^{(5)}$). Again, the rapid decrease of $\frac{\Delta_{68\%}}{\delta(X)^{(5)}}$ with the energy can be observed. The predictions based on the genuine set of the potential parameters S_0 , shown in the third column of Tab. I do not need to be in the centre of predictions obtained with various sets of the potential parameters. Thus in the 4th and the 5th columns of Tab. I we give distances between the predictions from the 3rd column and minimal and maximal predictions among those based on 34 sets of potential parameters taken into account when calculating $\Delta_{68\%}$. The different magnitudes of these distances, at the given energy and scattering angle, point to a nonlinear dependence of the 3N observables on the NN potential parameters.

Bayesian statistics also yields a general and statistically well-founded approach to quantify truncation errors in perturbative calculations. We employ here the same Bayesian procedure as already used by the LENPIC Collaboration to study truncation errors in NN and 3N scattering [12], which is a slightly modified version of the Bayesian approach developed in Refs. [13, 14]. Therefore, in the following we again only briefly describe our Bayesian procedure to determine the truncation errors and focus on a comparison of its results with the previously discussed statistical and truncation errors.

Rewriting Eq. (4.1) in terms of dimensionless expansion coefficients c_i in the form

$$X = X_{ref} (c_0 + c_2 Q^2 + c_3 Q^3 + c_4 Q^4 + \dots) , \quad (4.3)$$

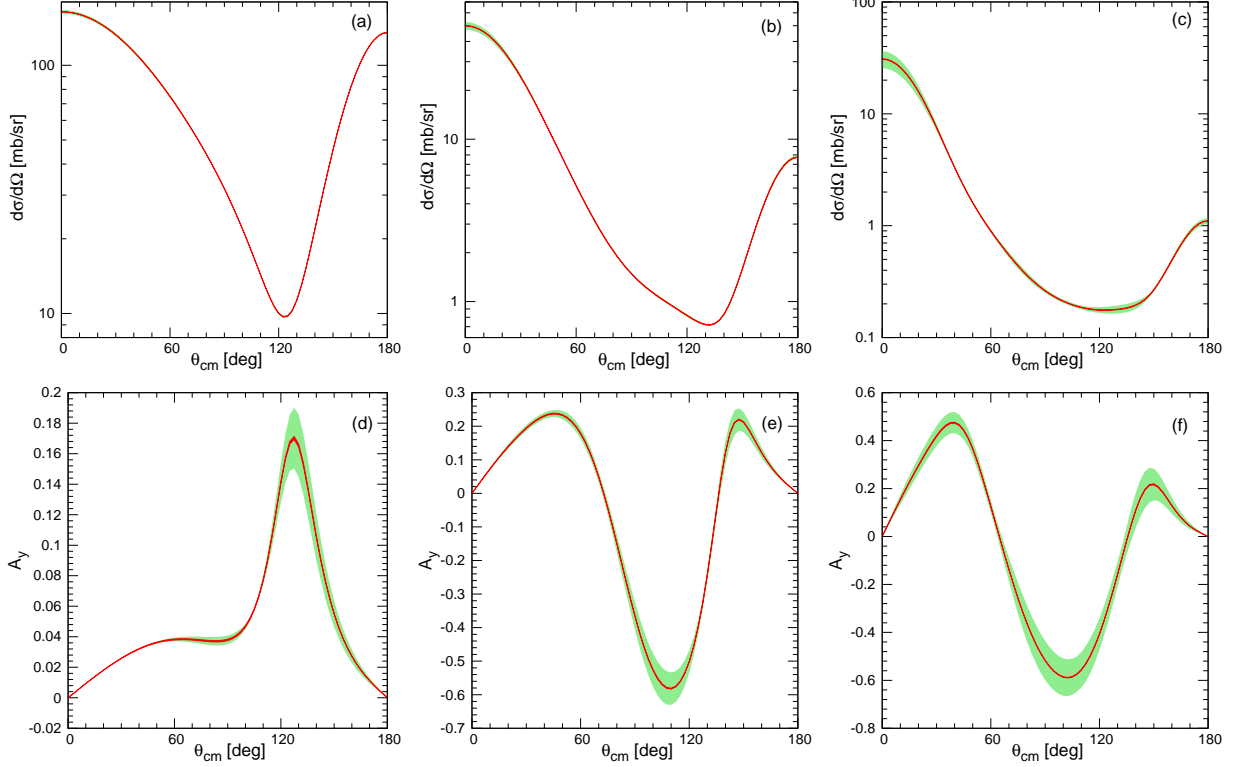


FIG. 7. (color online) Predictions for the differential cross section $d\sigma/d\Omega$ (top panels (a), (b) and (c)) and the neutron analyzing power A_y (bottom panels (d), (e) and (f)) for elastic nd scattering at the incoming neutron laboratory energy (a), (d) $E = 13$ MeV, (b), (e) $E = 65$ MeV and (c), (f) $E = 135$ MeV as a function of the center-of-mass scattering angle $\theta_{c.m.}$. The red and light-green bands denote the statistical uncertainty and 68% DoB interval using the Bayesian model $\bar{C}_{0.5-10}^{650}$ based on the chiral SMS N²LO ($\Lambda = 450$ MeV) NN potential, respectively.

setting the overall scale X_{ref} , with $\Delta X^{(i)}$ given in Eq. (4.2), as

$$X_{ref} = \begin{cases} \max(|X^{(0)}|, Q^{-2}|\Delta X^{(2)}|) & \text{for } k = 2, \\ \max(|X^{(0)}|, Q^{-2}|\Delta X^{(2)}|, Q^{-3}|\Delta X^{(3)}|) & \text{for } k \geq 3, \end{cases} \quad (4.4)$$

and assuming that $\Delta X^{(i)}$ are known explicitly up to the order $X^{(k)}$, $k \geq 2$, one can estimate the size of the truncation error at the k -th order of the chiral expansion as $\delta X_{Bayes}^{(k)} \equiv X_{ref} \Delta$ where $\Delta \equiv \sum_{i=k+1}^{\infty} c_i Q^i \approx \sum_{i=k+1}^{k+h} c_i Q^i$ is distributed, given the knowledge of $\{c_{i \leq k}\}$ with a posterior probability density function

$$\text{pr}_h(\Delta | \{c_{i \leq k}\}) = \frac{\int_0^{\infty} d\bar{c} \text{pr}_h(\Delta | \bar{c}) \text{pr}(\bar{c}) \prod_{i \in A} \text{pr}(c_i | \bar{c})}{\int_0^{\infty} d\bar{c} \text{pr}(\bar{c}) \prod_{i \in A} \text{pr}(c_i | \bar{c})}. \quad (4.5)$$

Here the prior probability density function $\text{pr}(c_i | \bar{c})$ is taken in the form of the Gaussian $N(0, \bar{c}^2)$ function and $\text{pr}(\bar{c})$ is a log-uniform distribution in the range (\bar{c}_-, \bar{c}_+) . Set A is defined as $A = \{n \in \mathbb{N}_0 \mid n \leq k \wedge n \neq 1 \wedge n \neq m\}$, $m \in \{0, 2, 3\}$ and

$$\text{pr}_h(\Delta | \bar{c}) \equiv \left[\prod_{i=k+1}^{k+h} \int_{-\infty}^{\infty} dc_i \text{pr}(c_i | \bar{c}) \right] \delta \left[\Delta - \sum_{j=k+1}^{k+h} c_j Q^j \right], \quad (4.6)$$

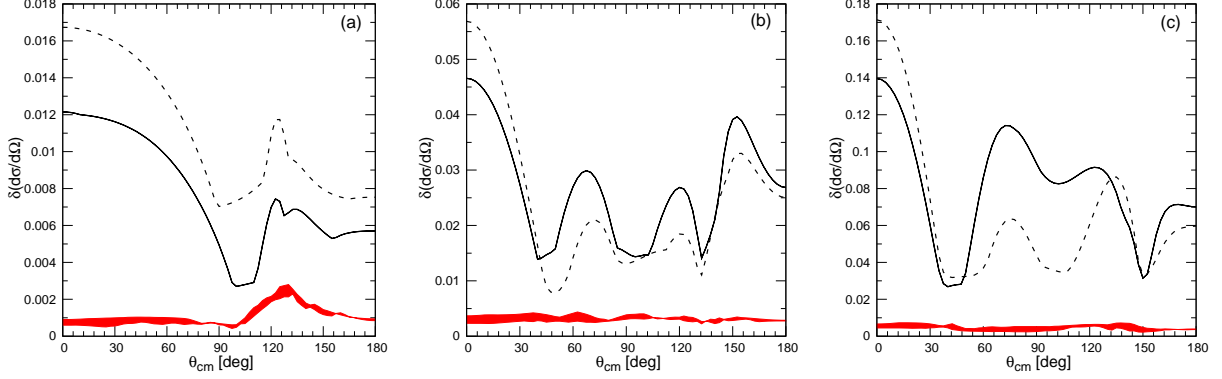


FIG. 8. (color online) The ratios $\delta(d\sigma/d\Omega) = \frac{E}{\frac{d\sigma}{d\Omega}|_{S_0}}$ with $E = \{\frac{1}{2}\Delta_{68\%}, \delta(X)^{(3)}, \delta(X)_{Bayes}^{(3)}\}$ that is the relative statistical uncertainties (the red band), the relative truncation errors (Eq. (4.2)) (the solid black curve) and the relative Bayesian truncation error from the $\bar{C}_{0.5-10}^{650}$ model (the dashed black curve), obtained with the SMS N²LO ($\Lambda = 450$ MeV) NN potential for the differential cross section $d\sigma/d\Omega$ in elastic nd scattering at the incoming nucleon laboratory energies: (a) $E = 13$ MeV, (b) $E = 65$ MeV and (c) $E = 135$ MeV as a function of the center-of-mass scattering angle $\theta_{c.m.}$.

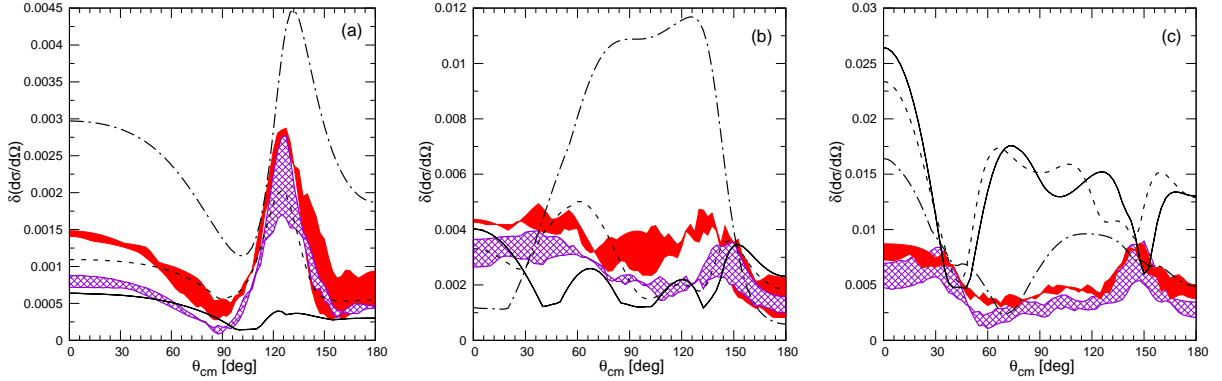


FIG. 9. (color online) The same ratios as in Fig.8 but for the chiral SMS N⁴LO ($\Lambda = 450$ MeV) NN potential. The additional dark-violet band represents the relative statistical uncertainty for the OPE-Gaussian potential. The additional black dash-dotted curve shows the ratio δ_{reg} measuring the cutoff dependence, see text.

with h being the number of the chiral orders above k which contribute to the truncation error. The resulting $\text{pr}_h(\Delta | \{c_{i \leq k}\})$ is symmetric with respect to $\Delta = 0$ so one can find the degree-of-belief (DoB) interval $(-d_k^{(p)}, d_k^{(p)})$ at the probability p , as a solution to the inverse problem given by the numerical integration

$$p = \int_{-d_k^{(p)}}^{d_k^{(p)}} \text{pr}_h(\Delta | \{c_{i \leq k}\}) d\Delta \quad (4.7)$$

and consequently the truncation error $\delta X_{Bayes}^{(k)} = X_{ref} d_k^{(p)}$. In the following we use $h = 10$, $\bar{c}_< = 0.5$, $\bar{c}_> = 10$, $\Lambda_b = 650$ MeV and $M_\pi^{eff} = 200$ MeV. The two latter quantities enter

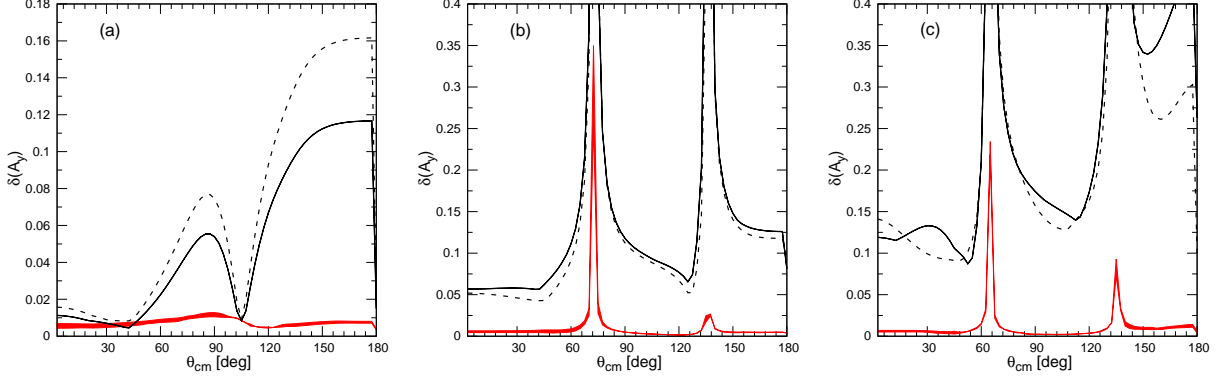


FIG. 10. (color online) The same ratios as in Fig.8 but for the neutron analyzing power A_y . The curves and bands are the same as in Fig. 8.

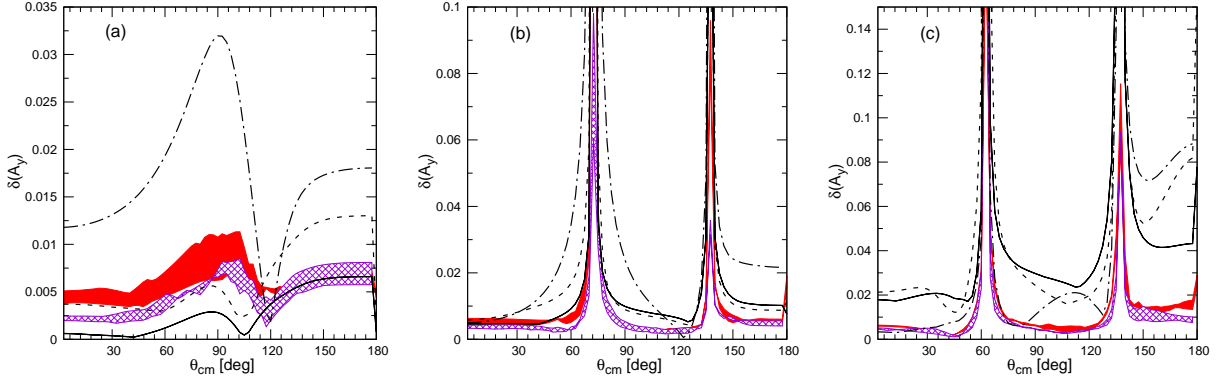


FIG. 11. (color online) The same ratios as in Fig.9 but for the neutron analyzing power A_y . The curves and bands are as in Fig. 9

the expansion parameter $Q = \max\left(\frac{p}{\Lambda_b}, \frac{M_\pi^{eff}}{\Lambda_b}\right)$ with momentum scale p defined in Eq.(17) of Ref. [12]. The detailed expression for $\text{pr}_h(\Delta | \{c_{i \leq k}\})$ for assumed priors can be found in Appendix A of Ref. [12] and our choice of the $h, \bar{c}_<, \bar{c}_>$ and Λ_b values corresponds to the model $\bar{C}_{0.5-10}^{650}$ from Ref. [12].

In Fig. 7 we show the differential cross section and the neutron analyzing power A_y in elastic neutron-deuteron scattering at N²LO at the laboratory energies $E = 13, 65$ and 135 MeV for the cutoff value $\Lambda = 450$ MeV, along with the truncation error corresponding to the 68% DoB interval and the statistical uncertainty obtained with the same force. For the differential cross section both types of errors almost overlap at $E = 13$ MeV but with the increasing energy the magnitude of 68% DoB interval from the $\bar{C}_{0.5-10}^{650}$ Bayesian model exceeds the statistical uncertainty at forward and backward scattering angles as well as at the minimum of the cross section. This is more noticeable for A_y . In this case the truncation error proves to be much bigger than the statistical uncertainty at all energies. This domination of truncation errors appears in specific ranges of the scattering angle for two lower energies and at the $E=135$ MeV the truncation errors exceed the statistical ones in the whole angular domain.

To facilitate more insight into the magnitudes of the theoretical uncertainties we compute

the ratios of the theoretical errors and the predictions based on the genuine set of the potential parameters (set S_0). They are presented in Figs. 8-11. Fig. 8 confirms findings from Fig. 7 (and from Figs. 5-6 for other observables and at N⁴LO), that the magnitude of the statistical uncertainty is much smaller than the truncation errors obtained within both methods. In the case of the chiral SMS N⁴LO potential shown in Fig. 9 one observes more complex relations between the two types of the relative errors. As can be seen in Figs. 9(a) and 9(b), for the differential cross section at $E = 13$ MeV and at $E = 65$ MeV, the magnitude of the statistical uncertainty is bigger or comparable to the magnitude of the truncation errors computed in the two approaches. In the same figure we show also the uncertainty due to using various values of the cutoff parameter when regularizing the potential, which is related to the truncation uncertainty discussed above. We define it for the observable X as $\delta_{reg} \equiv \frac{\frac{1}{2}(\max_j(X_j) - \min_j(X_j))}{X_2}$, where the subscript $j \in \{1, 2, 3, 4\}$ corresponds to different values of the cutoff parameter $\Lambda=400, 450, 500,$ and 550 MeV, respectively. For both lower energies the uncertainty related to the cutoff parameters is much bigger than the remaining theoretical errors. At $E=135$ MeV the relative errors for statistical uncertainties are smaller compared to the truncation ones. Thus we observe that at this energy the truncation errors become a dominant source of the total theoretical uncertainty for calculations within a given chiral force. This situation will likely change after applying higher-order contributions to the NN chiral force, what should reduce the truncation error. The magnitude of the truncation errors is, as expected, much smaller at N⁴LO than at N²LO and the magnitude of the statistical uncertainties remains similar at these two orders of the chiral expansion and at the same reaction energy. In Fig. 9 the statistical uncertainty for the chiral SMS N⁴LO results is also compared with the results based on the OPE-Gaussian force. The latter is slightly smaller than the statistical uncertainty of the chiral prediction in the whole range of the scattering angle. It is worth noting that the absolute values of the relative errors remain below 0.5%, 1.2% and 3% at $E=13, 65$ and 135 MeV, respectively. This proves the high quality of the SMS potential at N⁴LO and the reliability of predictions based on this interaction.

The relative statistical uncertainty from the chiral SMS N²LO potential is smaller than the relative truncation errors for the neutron analyzing power A_y at all three energies presented in Fig. 10. This picture is similar to the one for the differential cross section with the same interaction, shown in Fig. 8. Increasing order of the chiral expansion to N⁴LO, see Fig. 11, the magnitude of the relative statistical uncertainty for A_y hardly changes. It is also similar to the magnitude of the same ratio for the OPE-Gaussian-potential-based predictions. At $E = 13$ MeV and below $\theta_{c.m.} \approx 115^\circ$ the relative statistical error again is bigger than the relative truncation uncertainty. The truncation errors grow significantly for both higher energies as displayed in Figs. 11(b) and 11(c). The uncertainty related to the cutoff dependence, important at low and medium energies, is surpassed by the truncation errors at $E=135$ MeV. The magnitudes of all the types of the uncertainties for A_y at $E=13, 65,$ and 135 MeV remain below approx. 1.5%, 2%, and 4%, except for regions of the scattering angle where A_y reaches zero.

The estimation of theoretical uncertainty shown in this section bases on predictions of only NN interaction which are incomplete from the third order of the chiral expansion, where the three-nucleon interaction starts to contribute. It is very likely that the estimated truncation errors will change after inclusion of the 3NF. This should be tested as soon as a 3NF consistent with the SMS NN potential is available.

V. RESULTS FOR THE DEUTERON BREAKUP REACTION

In the case of the neutron induced deuteron breakup reaction, we have selected a few kinematical complete configurations to exemplify only the statistical uncertainties for observables in this process.

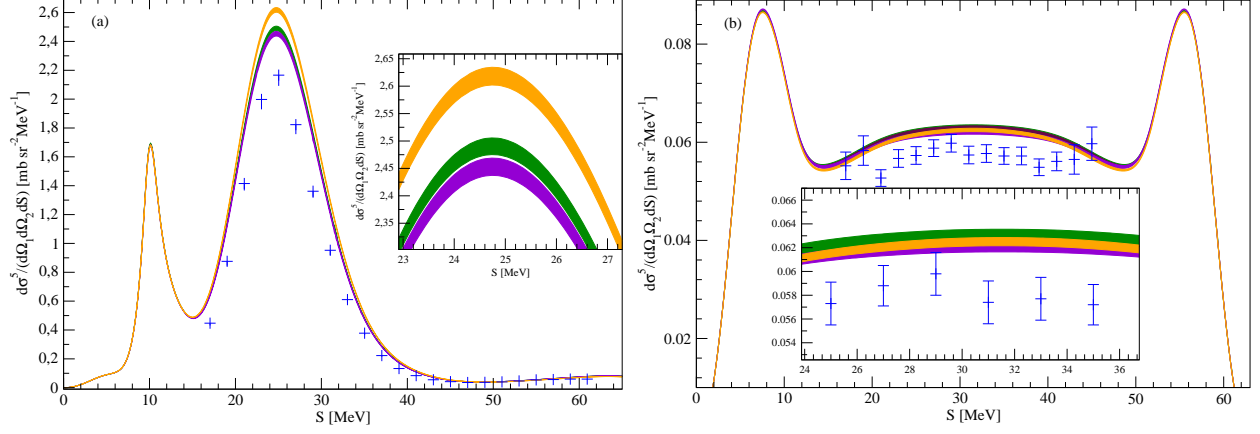


FIG. 12. The five-fold cross section $\frac{d^5\sigma}{d\Omega_1 d\Omega_2 dS}$ for the $d(n, n_1 n_2)p$ breakup reaction at the incoming nucleon laboratory energy $E=65$ MeV shown as a function of the arc-length S for the following polar angles θ_i and the relative azimuthal angle ϕ_{12} of the momenta of two detected neutrons: (a) $\theta_1 = 30.5^\circ, \theta_2 = 59.5^\circ, \phi_{12} = 180^\circ$ (QFS configuration) and (b) $\theta_1 = \theta_2 = 54.0^\circ, \phi_{12} = 120^\circ$ (SST configuration). The orange, green and violet bands represent statistical uncertainties obtained with the OPE-Gaussian force, the chiral N^4LO and N^4LO^+ ($\Lambda = 450$ MeV), respectively. The experimental proton-deuteron data are from Ref. [47] for (a) and from Ref. [48] for (b).

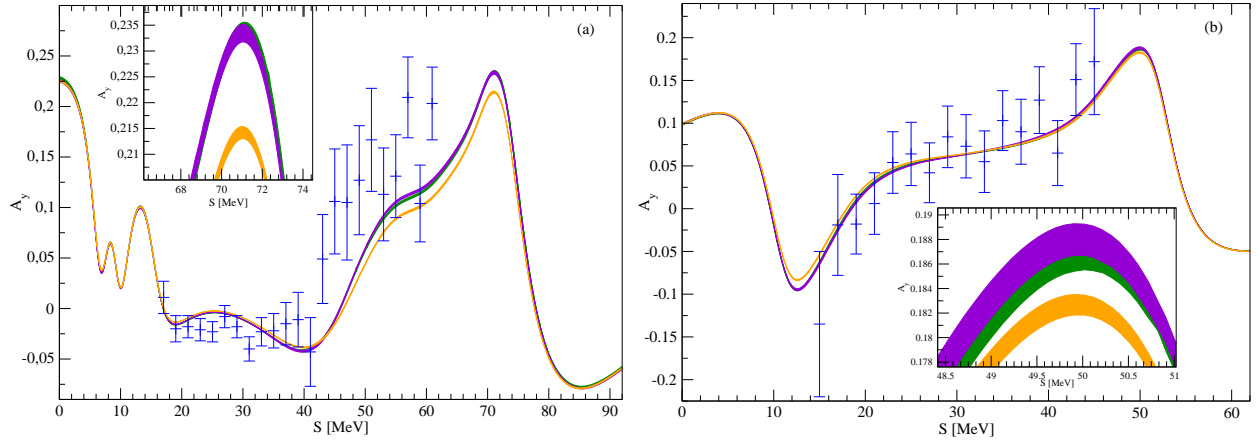


FIG. 13. The neutron analyzing power $A_y(n)$ for the $d(n, n_1 n_2)p$ breakup reaction at the incoming nucleon laboratory energy $E=65$ MeV for the following polar angles and the relative azimuthal angle of the momenta of two detected neutrons: (a) $\theta_1 = 30.5^\circ, \theta_2 = 59.5^\circ, \phi_{12} = 180^\circ$ and (b) $\theta_1 = \theta_2 = 54.0^\circ, \phi_{12} = 120^\circ$. The curves and bands as in Fig. 12. The proton-deuteron data are from Ref. [47].

Proceeding in the same way as for elastic nd scattering, we estimate the theoretical statistical uncertainties of nd breakup observables, due to uncertainty of the SMS NN po-

tential parameters. We show in Fig. 12 these uncertainties for the neutron-induced deuteron breakup cross section obtained with the chiral SMS potential with $\Lambda = 450$ MeV, at two orders of the chiral expansion, $N^4\text{LO}$ and $N^4\text{LO}^+$, and compare them with the corresponding results obtained with the OPE-Gaussian interaction. The magnitudes of the statistical uncertainties for the cross section reach their maximum approximately at $S = 25$ MeV for the quasi-free scattering (QFS) configuration in Fig. 12a. Predictions obtained with the chiral $N^4\text{LO}$ and $N^4\text{LO}^+$ potentials (at $\Lambda = 450$ MeV) differ slightly each other but the OPE-Gaussian force based results are clearly separated from the two chiral predictions. For the space-star configuration (SST) (Fig. 12b) the predictions of three potentials practically overlap. In Figs. 13a and 13b we exemplify the neutron analyzing power for the QFS and

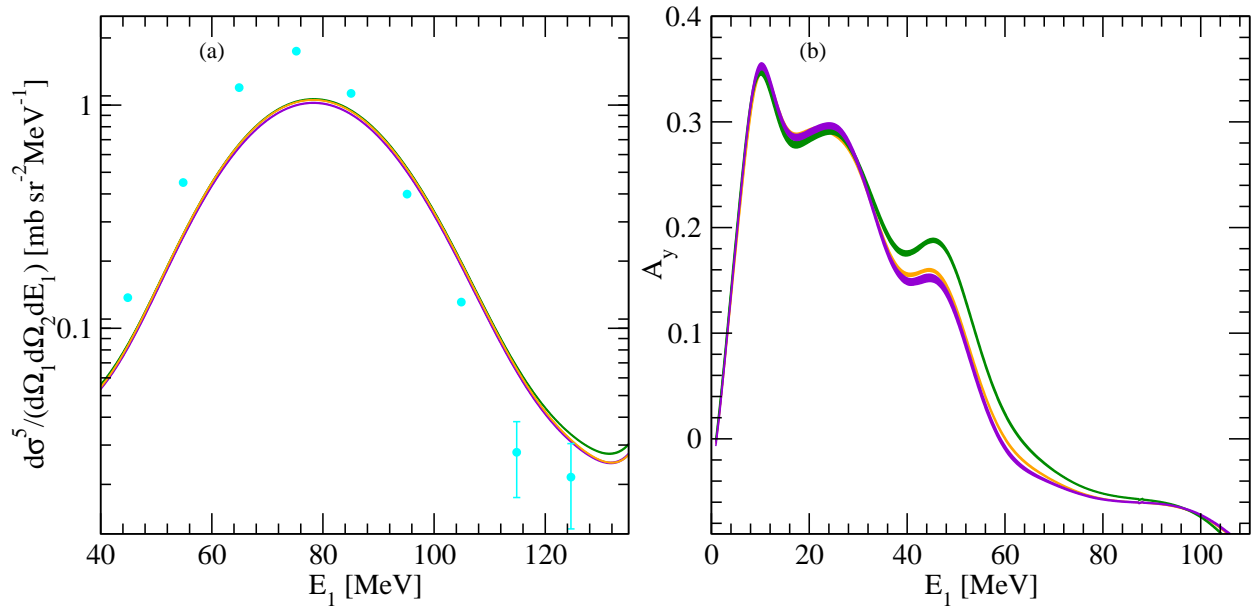


FIG. 14. (color online) (a) The five-fold differential cross section $\frac{d^5\sigma}{d\Omega_1 d\Omega_2 dE_1}$ as a function of the laboratory kinetic energy E_1 of the first detected nucleon for the following detection angles of two neutrons: $\theta_1 = 45.0^\circ, \theta_2 = 35.0^\circ, \phi_{12} = 180^\circ$ and (b) the neutron analyzing power for the $d(n, n_1 n_2)p$ breakup reaction as a function of the laboratory kinetic energy E_1 of the first detected nucleon for the following detection angles of two neutrons $\theta_1 = 52.0^\circ, \theta_2 = 45.0^\circ, \phi_{12} = 180^\circ$. The incoming neutron laboratory kinetic energy is $E=200$ MeV. The curves and bands are as in Fig. 12. The experimental proton-deuteron data in (a) are from Ref. [49].

SST configurations at $E = 65$ MeV, respectively. Here the statistical uncertainties remain negligible for both configurations. The differences between predictions based on the OPE-Gaussian force and the chiral potentials at $N^4\text{LO}$ and $N^4\text{LO}^+$ amount up to 7% as seen in the maximum of the $A_y(n)$ for the SST configuration. Fig. 14 exemplifies that at the higher energy $E = 200$ MeV the statistical uncertainties remain small. It is also interesting to note that for the breakup process there exist kinematical configurations for which a clear difference between chiral predictions at $N^4\text{LO}$ and $N^4\text{LO}^+$ is observed. This is exemplified in Fig. 14b, where the difference between results for the nucleon analyzing power around $E_1=48$ MeV at these two orders of the chiral expansion reaches $\approx 20\%$.

VI. SUMMARY AND CONCLUSIONS

We employed the new high-quality χ EFT NN potential with the semi-local regularization in momentum space at different orders of chiral expansion up to $N^4\text{LO}^+$ to describe the elastic nd scattering and the neutron-induced breakup reactions at energies up to 200 MeV. We used the correlation matrix of that NN potential parameters to study the propagation of uncertainties from the NN potential parameters to 3N observables. Next we compared these uncertainties with the truncation errors estimated using two different approaches: the prescription from Ref. [9] and the Bayesian approach from Refs. [12–14]. We calculated also the uncertainty of predictions induced by different values of the regularization cutoff parameter used.

The description of the data delivered by the chiral force with the semi-local momentum-space regularization is similar to that based on the older versions of the chiral potential from the Bochum-Bonn group. Our findings confirm that the statistical uncertainties of the elastic nd scattering observables are smaller than the dispersion of results arising from using various orders of chiral NN interactions, both at low- and at high-energies. We find that statistical errors remain still relatively small in the deuteron breakup process at the considered kinematical configuration independently from the employed NN force model. The statistical uncertainties of the chiral predictions have similar magnitudes and the energy dependence as those from the semi-phenomenological OPE-Gaussian force.

Clearly, at low and medium energies the regulator dependence dominates other types of uncertainties. Also the truncation errors found in our studies are not negligible. Only at low energies and at $N^4\text{LO}$ truncation errors become smaller than statistical uncertainties, both for the cross section and the neutron analyzing power. However, the estimated magnitudes of all types of uncertainties remain small, usually in the range 0.5%-4%, depending on the energy and the observable. The fact that various contributions to the theoretical uncertainty are so small points to the high quality of the theoretical input in the SMS interaction.

Summarizing, our analysis of theoretical uncertainties in the neutron-deuteron scattering confirms the SMS chiral potential belongs to the first-rate models of nuclear forces. It also demonstrates that, with an ongoing progress in the derivation, regularization and inclusion of higher-order contributions to the nuclear interaction, theoretical uncertainties, obtained with the chiral interaction, would be reduced to the limit dependent only on the quality of experimental data which influence the statistical errors. Presently this is observed for a fixed value of the regulator parameter only at low energies but very likely this region will be extended to much higher energy values.

ACKNOWLEDGMENTS

This work is a part of the LENPIC project and was supported by the Polish National Science Centre under Grants No. 2016/22/M/ST2/00173 and No. 2016/21/D/ST2/01120. It was also supported in part by BMBF (Grant No. 05P18PCFP1) and by DFG through funds provided to the Sino-German CRC 110 Symmetries and the Emergence of Structure in QCD (Grant No. TRR110). Numerical calculations were performed on the supercomputer

cluster of the JSC, Jülich, Germany.

- [1] Epelbaum E, Hammer H W and Meißner U-G 2009 *Rev. Mod. Phys.* **81** 1773
- [2] Epelbaum E and Meißner U-G 2012 *Ann. Rev. Nucl. Part. Sci.* **62** 159
- [3] Machleidt R and Entem D R 2011 *Phys. Rept.* **503** 1
- [4] Epelbaum E, Krebs H and Reinert P 2019 arXiv:1911.11875 [nucl-th]
- [5] Piarulli M and Tews I, arXiv:2002.00032 [nucl-th]
- [6] Epelbaum E, Krebs H and Meißner U-G 2015 *Eur. Phys. J. A* **51** 53
- [7] Epelbaum E, Krebs H and Meißner U-G 2015 *Phys. Rev. Lett.* **115** 122301
- [8] Binder S *et al.* [LENPIC Collaboration] 2016 *Phys. Rev. C* **93**, 044002
- [9] Binder S *et al.* [LENPIC Collaboration] 2018 *Phys. Rev. C* **98**, 014002
- [10] Reinert P, Krebs H and Epelbaum E 2018 *Eur. Phys. J. A* **54** 86
- [11] Epelbaum E *et al.* 2019 *Phys. Rev. C* **99** 024313
- [12] Epelbaum E *et al.* 2019 arXiv:1907.03608 [nucl-th]
- [13] Furnstahl R J, Klco N, Phillips D R and Wesolowski S 2015 *Phys. Rev.* **92** 024005
- [14] Melendez J A Wesolowski S Furnstahl R J 2017 *Phys. Rev. C* **96** 024003
- [15] Ekström A *et al.* 2013 *Phys. Rev. Lett.* **110** 192502
- [16] Ireland D G and Nazarewicz W J 2015 *Phys. G: Nucl. Part. Phys.* **42** 030301 and references therein
- [17] Kalantar-Nayestanaki N, Epelbaum E, Messchendorp J G, Nogga A 2012 *Rep. Prog. Phys.* **75** 016301
- [18] Machleidt R 2001 *Phys. Rev. C* **63** 024001
- [19] Wiringa R B, Stoks V G J and Schiavilla R 1995 *Phys. Rev. C* **51** 38
- [20] Entem D R, Machleidt R and Nosyk Y 2017 *Phys. Rev. C* **96** 024004
- [21] Maria Piarulli *et al.* 2015 *Phys. Rev. C* **91** 024003
- [22] Maria Piarulli *et al.* 2016 *Phys. Rev. C* **94** 054007
- [23] Pérez R Navarro Amaro J E and Arriola E Ruiz 2013 *Phys. Rev. C* **88**, 064002
- [24] Pérez R Navarro, Garrido Amaro J E and Arriola E Ruiz 2014 *Phys. Rev. C* **89** 064006
- [25] Pérez R Navarro, Amaro J E and Arriola E Ruiz 2015 *J. Phys. G: Nucl. Part. Phys.* **42** 034013
- [26] Skibiński R *et al.* 2018 *Phys. Rev. C* **98** 014001
- [27] Glöckle W *et al.* 1996 *Phys. Rept.* **274** 107
- [28] Witała H *et al.* 2001 *Phys. Rev. C* **63** 024007 (2001)
- [29] Sekiguchi K *et al.* *Phys. Rev. C* **96** 064001 (2017)
- [30] Glöckle W 1983 *The Quantum-Mechanical Few-Body Problem. Springer-Verlag, Berlin*
- [31] Ermisch K *et al.* 2005 *Phys. Rev. C* **71** 064004
- [32] Pérez R Navarro, Garrido E Amaro J E and Arriola E Ruiz 2014 *Phys. Rev. C* **90** 047001 (2014)
- [33] Pérez R Navarro *et al.* 2015 *J. Phys.: Conf. Ser.* **742** 012001 (2016)
- [34] Deltuva A, Fonseca A C, Sauer P U 2006 *Phys. Rev. C* **73** 057001
- [35] Shimizu S *et al.* 1995 *Phys. Rev. C* **52** 1193
- [36] Rühl H *et al.* 1991 *Nucl. Phys. A* **524** 377
- [37] Sekiguchi K *et al.* 2005 *Phys. Rev. Lett.* **95** 162301
- [38] Sakamoto N *et al.* 1996 *Phys. Lett. B* **367** 60; Sakai H *et al.* 2000 *Phys. Rev. Lett.* **84** 5288
- [39] Sekiguchi K *et al.* 2002 *Phys. Rev. C* **65** 34003

- [40] Adelberger R E and Brown C N 1972 *Phys. Rev. D* **5** 2139
- [41] Igo G *et al.* 1972 *Nucl. Phys. A* **195** 33
- [42] Przewoski B v *et al.* 2006 *Phys. Rev. C* **74** 064003
- [43] Cadman R V *et al.* 2001 *Phys. Rev. Lett.* **86** 967
- [44] Witala H *et al.* 1993 *Few-Body Syst.* **15** 67
- [45] Stephan E *et al.* 2007 *Phys. Rev. C* **76** 057001
- [46] Mardanpour H *et al.* 2007 *Eur. Phys. J. A* **31** 383
- [47] Allet M *et al.* 1996 *Few-Body Syst.* **20** 27
- [48] Zejma J *et al.* 1997 *Phys. Rev. C* **55** 42
- [49] Pairsuwan W, Watson J W, Ahmad M, Chant N S, Flanders B S, Madey R, Pella P J, Roos P G 1995 *Phys. Rev. C* **52** 2552